Research Article

Journal of PeptideScience

Received: 7 October 2015 Revised: 6 November 2015 Accepted: 11 November 2015 Published online in Wiley Online Library: 18 December 2015

(wileyonlinelibrary.com) DOI 10.1002/psc.2842

The crystal structure of Z-$(Aib)_{10}$-OH at 0.65 Å resolution: three complete turns of 3_{10}-helix

Renate Gessmann,[a] Hans Brückner[b] and Kyriacos Petratos[a]*

The synthetic peptide Z-$(Aib)_{10}$-OH was crystallized from hot methanol by slow evaporation. The crystal used for data collection reflected synchrotron radiation to sub-atomic resolution, where the bonding electron density becomes visible between the non-hydrogen atoms. Crystals belong to the centrosymmetric space group $P\bar{1}$. Both molecules in the asymmetric unit form regular 3_{10}-helices. All residues in each molecule possess the same handedness, which is in contrast to all other crystal structure determined to date of longer Aib-homopeptides. These other peptides are C-terminal protected by O*t*Bu or OMe. In these cases, because of the missing ability of the C-terminal protection group to form a hydrogen bond to the residue i-3, the sense of the helix is reversed in the last residue. Here, the C-terminal OH-groups form hydrogen bonds to the residues i-3, in part mediated by water molecules. This makes Z-$(Aib)_{10}$-OH an Aib-homopeptide with three complete 3_{10}-helical turns in spite of the shorter length it has compared with Z-$(Aib)_{11}$-O*t*Bu, the only homopeptide to date with three complete turns.

Additional supporting information may be found in the online version of this article at the publisher's web site.

Keywords: α-aminoisobutyric acid; 3_{10}-helix; sub-atomic resolution; centrosymmetry; achiral peptide; left-handed helix; unprotected peptide; three complete turns

Introduction

The conformational space available to α-amino-isobutyric acid (Aib) residues is severely restricted by the second methyl group attached to the Cα atom. This space comprises the left-handed and right-handed helical region of the Ramachandran plot. Aib residues are known as strong helix formers in peptides, also in the presence of common amino acids [1–3]. Helical conformation is a prerequisite for the formation of pores by self-association of naturally occurring peptides rich in Aib-residues (e.g. peptaibols) in lipid bilayer membranes [4]. Peptides consisting of only Aib residues show a clear preference for left-handed and right-handed 3_{10}-helices in solution and crystal structures. All crystal structures of Aib homopeptides known to date [5–14] show the following common properties: centrosymmetric space group, regular 3_{10}-helices with the maximum number of hydrogen bonds involving also the *N*-terminal protecting group, head-to-tail hydrogen-bonded columns and a reversal of the helical sense at the C-terminal residue. The latter was not observed for Z-$(Aib)_3$-OH anhydrate and monohydrate [5]. Apart from these two peptides, only Z-$(Aib)_4$-OH and Z-$(Aib)_5$-OH [6] were investigated by crystallography as C-unblocked homopeptides, and in both the sense of the helix was found reversed at the last residue. All other structures of Aib-homopeptides are protected at the C-terminal with OMe (methoxy) or O*t*Bu (*tert*-butoxy) groups, which interrupt the helical hydrogen bonding scheme by replacing the hypothetical following NH-group with oxygen. The latter replacement results in unfavourable short distance between the oxygen of the protecting group and the C=O group of residue i-3, and it is avoided by reversing the backbone in the opposite direction. These findings lead us to investigate the C-terminal conformation in the long, C-unblocked Aib10. Furthermore, the only structure available of a $(Aib)_{10}$ peptide contains the heavy bromine (Z=35) incorporated at the N-terminus, which was found to affect the crystal packing and hence the resulting structure. This renders the latter structure not comparable with the other homopeptides. Finally, the easily tunable wavelength at the microfocus beamline I-24 at the British synchrotron (Diamond) enabled data collection in the sub-atomic resolution of 0.65 Å.

Materials and methods

Synthesis and crystallization

The protected decapeptide Z-$(Aib)_{10}$-O*t*Bu was synthesized by heating of Z-Aib_5-Ox (5.38 g, 9.61 mmol) (Ox refers to the oxazolone formed from the C-terminal Aib of the Z-protected pentapeptide on reaction with acetic anhydride for 1.5 h at 100 °C) with H-$(Aib)_5$-O*t*Bu (4.80 g, 9.61 mmol) in 150 ml butyronitrile for 26 h at 100 °C. The solvent was evaporated *in vacuo*; the remaining residue

* *Correspondence to: Kyriacos Petratos, IMBB/FORTH, 70013 Iraklion Crete, Greece. E-mail: petratos@imbb.forth.gr*

a *IMBB/FORTH, 70013, Iraklion Crete, Greece*

b *Department of Food Sciences, Interdisciplinary Research Center, Justus-Liebig-University of Giessen, 35392, Giessen, Germany*

Abbreviations: *Z, benzyloxycarbonyl; OMe, methoxy; OtBu, tert butoxy; Aib, α-aminoisobutyric acid; Ox, oxazonon.*

Journal of PeptideScience

dissolved in 250 ml chloroform, and washed three times with 200 ml $KHSO_4$ (5%), $KHCO_3$ and water. The organic phase was dried with Na_2SO_4, and evaporated to dryness. The peptide was dissolved in hot chloroform and crystallized by addition of light petroleum (b.p. 40–60 °C). Yield 7.74 g (76%), m.p. 252–255 °C, $r_F = 0.27$ (mobile phase ethyl acetate, distance start to solvent front 17.5 cm, pre-coated silica plate from Merck, 20 × 20 cm). Positive mode electrospray ionization mass spectrum: *m/z* 1081.46 $[M+Na]^+$, 1059.13 $[M+H]^+$, and regular series of acylium fragment ions differing by 85.1 mass units (Aib - H_2O) ranging from *m/z* 304.87 (b_2) to *m/z* 985.29 (b_{10}) [15,16]. To Z-(Aib)$_{10}$O*t*Bu (4.30 g, 4.06 mol) in dichloro-methane (10 ml) trifluoroacetic acid (80 ml) was added and the mixture stirred at room temperature for 2 h. Solvents were removed *in vacuo*, the remaining residue dissolved in MeOH and the decapeptide carboxylic acid precipitated by addition of diethyl ether. $r_F = 0.62$ (mobile phase chloroform/methanol 85:15, v/v, distance start to solvent front 7.5 cm, pre-coated silica plate from Merck, 5 × 10 cm). Z-(Aib)$_{10}$-OH was dissolved in hot methanol and crystallized by slow evaporation. Crystals were visible after a few days.

Data collection

One single plate with the smallest dimension of about 25 μm was mounted on a cryoloop without cryoprotectant and kept in place with a minimal amount of vacuum grease (Supporting Information Figure S1). Diffraction data were collected at 100 K on the microfocus beamline I24 [17] of Diamond Light Source in Didcot, England using a Pilatus 6 M detector (Dectris Ltd, Baden, Switzerland). A dataset of 1800 images covering 360° of rotation was collected from a single crystal. The data were integrated using the software package *XDS* [18] and scaled with *AIMLESS* [19] implemented in the *CCP4* suite [20].

The dataset statistics are summarized in Table 1. Although the data were collected to a nominal resolution of 0.63 Å, the processed data were limited to 0.65 Å resolution because of the very low completeness beyond 0.65 Å.

Table 1. Data collection and processing. Values in parentheses are for the outermost resolution shell

Crystal data	
Chemical formula	$C_{48}O_{13.57}N_{10}H_{78.9}$
M_r	1013.31
Crystal system, space group	Triclinic, $P\,\overline{1}$
Temperature (K)	100
a, *b*, *c* (Å)	15.784 (8), 18.424 (7), 20.999 (12)
α, β, γ (°)	107.768 (6), 91.626 (4), 103.158 (15)
V (Å^3)	5631 (5)
Z	4
Wavelength (Å)	$\lambda = 0.59039$
Resolution range (Å)	19.9–0.65 (0.7–0.65)
μ (mm^{-1})	0.03
Crystal size (mm)	0.12 × 0.12 × 0.025
No. of measured reflections	107 673 (4186)
No. of unique reflections	31 118 (1749)
Mean $I/\sigma(I)$	9.6(4.3)
Completeness (%)	72.5(20.5)
R_{pim}[$] (%)	4.4(15.4)
R_{meas}* (%)	8.2(21.3)
Final R_{cryst}, R_{crys} $F_o > 4\sigma F_o$ (%)	9.04, 8.23
Final R_{free}, R_{free} $F_o > 4\sigma F_o$ (%)	10.13, 9.25
No. of all unique reflections	31 118
No. of reflections for R_{free}	1568
No. of parameters	1504
No. of restraints	371
Average B-factor[#] (Å^2)	
mol A main/side chain	3.2/4.8
mol B main/side chain	2.9/4.2

[$] $R_{pim} = \Sigma(1/(N-1))^{1/2} \cdot |I - <I>|/\Sigma I$, N = number of symmetry related reflections.

* $R_{meas} = \Sigma(N/(N-1))^{1/2} \cdot |I - <I>|/\Sigma I$.

[#] Non-hydrogen atoms.

Structure solution and refinement

The structure was solved by direct methods with *SHELXS86* [21]. All 142 non-hydrogen atoms of two peptide molecules termed hereafter mol A and mol B, and one water oxygen atom could be located in the first electron density map as highest peaks. The structure was refined using the program *SHELXL* [21].

During refinement, one disorder of the N-terminus of mol A comprising seven non-hydrogen atoms, disorders of the last residue of both molecules and a disorder of one methyl group of Aib 5 in mol B were detected, which were described as the second components in different conformation. Interestingly, the next high peaks in the electron density maps of the initial structure solution proved to be the oxygen atoms of the second C-terminal conformation of mol B. Several restraints were introduced to improve the geometry and the thermal parameters of these disordered residues. Both

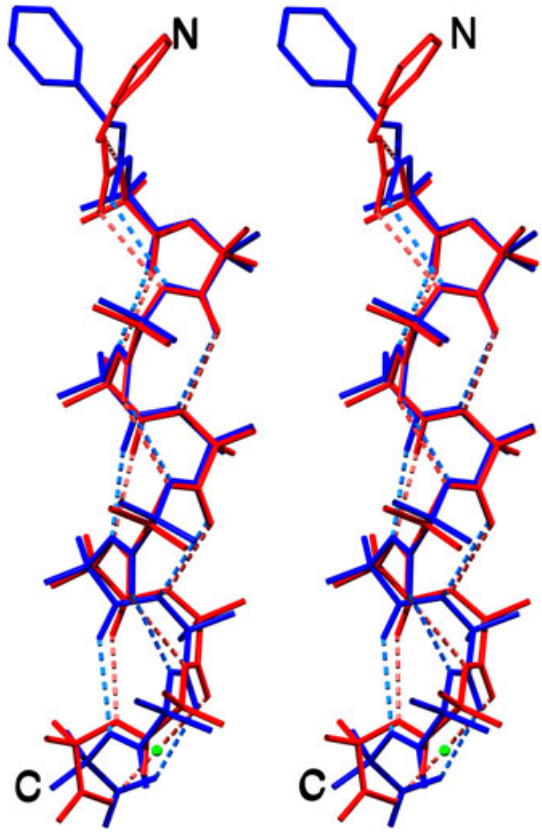

Figure 1. Wall-eyed stereo view of the superposition of mol B (blue) on mol A (red), the water molecule is shown as a green sphere. Hydrogen bonds appear in orange for mol A and light blue for mol B. N and C denote the amino-termini and carboxyl-termini of the molecules. For clarity, only the main conformations are shown.

equally occupied conformations of the Z-protection group of mol A were refined to be almost at the same position after the application of anisotropic refinement. There was also a clear appearance of negative electron density at the atom ring positions. The latter observations obliged us to refine these regions isotropically. Hydrogens were added in calculated positions and refined as riding with the thermal displacement parameters fixed to 1.5 (for methyl hydrogens) and 1.2 (for all others) times of the isotropic displacement parameter of the parent atom. The torsion angles of the C-terminal hydrogens were allowed to refine, and because of the low occupancy and the resulting estimated high standard deviations the maximum shift/error of 1.36 remains for the second conformations in the last cycles of refinement. Experimental details are listed in Table 1. *Xtalview* [22], *Swiss PDBViewer* [23], *Coot* [24], *Ortep-3* [25], *Pymol* [26] and *POV-Ray* [27] were used for geometric analysis, visualization and for the production of the figures.

Accession number

The coordinates and structure factors have been deposited with the Cambridge Data Bank [28] under accession code CCDC 1430000. These data can be obtained from The Cambridge Crystallographic Data Centre via www.ccdc.cam.ac.uk/data_request/cif.

Table 2. Backbone torsion angles for the right handed molecules

Angle(°)	Mol A	2nd conf.	Mol B	2nd conf.
$\zeta 2(Z)$	151.2(7)	148.1(4)	−130.3(2)	—
$\zeta 3(Z)$	−166.0(7)	−174.8(3)	−23.3(3)	—
$\omega(Z)$	−177.3(2)	−178.5(2)	−177.3(2)	—
$\varphi(1)$	−57.1(2)	—	−56.5(2)	—
$\psi(1)$	−30.5(2)	—	−29.8(2)	—
$\omega(1)$	−179.6(2)	—	−178.1(2)	—
$\varphi(2)$	−47.9(2)	—	−50.7(2)	—
$\psi(2)$	−40.1(2)	—	−35.8(2)	—
$\omega(2)$	−173.1(1)	—	−174.8(1)	—
$\varphi(3)$	−56.7(2)	—	−54.2(2)	—
$\psi(3)$	−30.2(2)	—	−31.9(2)	—
$\omega(3)$	−177.8(1)	—	−177.8(1)	—
$\varphi(4)$	−58.6(2)	—	−55.6(2)	—
$\psi(4)$	−19.0(2)	—	−24.5(2)	—
$\omega(4)$	−173.6(1)	—	175.1(2)	−175.1(7)
$\varphi(5)$	−48.9(2)	—	−48.0(5)	−62.4(15)
$\psi(5)$	−34.1(2)	—	−34.8(8)	−21.6(22)
$\omega(5)$	−176.8(1)	—	−174.7(4)	177.0(10)
$\varphi(6)$	−52.6(2)	—	−55.4(5)	−49.7(13)
$\psi(6)$	−32.7(2)	—	−29.6(2)	—
$\omega(6)$	−178.6(1)	—	−177.3(1)	—
$\varphi(7)$	−53.3(2)	—	−51.1(2)	—
$\psi(7)$	−34.2(2)	—	−32.4(2)	—
$\omega(7)$	−175.5(1)	—	−177.8(1)	—
$\varphi(8)$	−53.7(2)	—	−54.5(2)	—
$\psi(8)$	−32.8(2)	—	−25.5(2)	—
$\omega(8)$	−177.5(1)	—	−179.9(1)	—
$\varphi(9)$	−64.2(3)	−56.9(20)	−50.6(2)	—
$\psi(9)$	−16.3(3)	−10.5(47)	−29.3(3)	−40.5(10)
$\omega(9)$	−157.8(2)	160.33(35)	174.8(3)	−151.5(12)
$\varphi(10)$	−51.7(3)	−50.9(44)	−51.4(5)	−33.1(22)
$\psi(10)$	−49.5(3)	−39.5(33)	−33.8(4)	−59.9(20)

* The angles $\zeta 2(Z)$, $\zeta 3(Z)$ and $\omega(Z)$ are defined as C1-C7-O7-C, C7-O7-C-N(1) and O7-C-N(1)-Cα(1), respectively, and $\psi(10)$ is the angle N(10)-CA(10)-C(10)-O (of group OH 10).

Results and discussion

Two independent molecules (mol A and mol B) were located in the crystal's asymmetric unit. Figure 1 shows a superposition of the two independent molecules (main conformations only). The rms-deviation of all atoms is 0.96 Å with the maximum of 3.2 Å at the C-termini, while the rms-deviation of main chain atoms is 0.57 Å with a maximum of 2.4 Å. Both molecules possess a higher flexibility at both ends. This is reflected by the second conformations and

Table 3. Hydrogen-bond geometry (Å,°)

D–H···*A*	H···*A*	*D*···*A*	*D*–H···*A*	N···O = C
intramolecular, mol A				
N_3–H_3···O(Z)	2.15	2.968(2)	154.5	130.5(1)
N_4–H_4···O_1	2.14	2.951(2)	152.6	131.2(1)
N_5–H_5···O_2	2.16	3.014(2)	163.0	129.4(1)
N_6–H_6···O_3	2.07	2.931(2)	165.7	132.2(1)
N_7–H_7···O_4	2.11	2.925(2)	154.3	129.0(1)
N_8–H_8···O_5	2.11	2.925(2)	154.3	131.7(1)
N_9–H_9···O_6	2.23	3.032(3)	151.0	126.9(1)
N_10^1–H_10^1···O_7	2.09	2.913(3)	155.8	128.9(1)
N_10^2–H_10^2···O_7	2.24	3.098(20)	166.6	129.3(3)
mol B				
N_3–H_3···O(Z)	2.18	3.021(2)	159.1	129.3(1)
N_4–H_4···O_1	2.14	2.961(2)	154.0	131.7(1)
N_5–H_5···O_2	2.13	2.960(2)	157.4	131.4(1)
N_6–H_6···O_3	2.10	2.960(2)	166.4	132.0(1)
N_7–H_7···O_4	2.14	2.986(2)	160.7	130.1(1)
N_8^3–H_8^3···O_5	2.25	3.094(8)	161.1	132.1(5)
N_8^4–H_8^4···O_5	2.05	2.901(23)	164.0	132.1(16)
N_9–H_9···O_6	2.10	2.960(2)	165.0	132.8(1)
N_10^3–H_10^3···O_7	2.21	3.062(5)	162.5	133.7(2)
N_10^4–H_10^4···O_7	2.06	2.916(2)	163.8	130.9(4)
O_10^4–H_10^4···O_8	1.96	2.755(3)	157.3	136.2(1)
intermolecular A to B				
N_1–H_1···O_9^{i}	2.03	2.903(2)	173.2	167.0(2)
B to A				
N_1–H_1···$O\_9^{ii,1}$	1.91	2.777(2)	169.4	160.8(2)
N_1–H_1···O_9^2	2.01	2.862(16)	161.6	143.9(16)
N_2–H_2···O_10^1	2.25	3.108(3)	164.5	109.4(2)
mol A to water 1				
H_2O1^1–$H2^1$···O_8	1.83	2.871(3)	170.1	129.3(1)
OH_10^1–HH_10^1···H_2O1^1	1.84	2.610(1)	151.1	127.3(1)
mol B to water 1				
H_2O1^1–$H1^1$···O_10^3	2.24	3.118(4)	174.8	130.8(3)
mol B to water 2				
$HOH2^2$···O_8	—	2.881(23)	—	127.4(6)
OH_10^2–HH_10^2···H_2O2^2	1.88	2.627(84)	146.9	119.1(17)
mol A to water 2				
H_2O2^2···$O\_10^{iii,2}$	—	3.072(35)	—	133.2(31)

The numbers denote disordered atoms with occupancies (1) 0.9; (2) 0.1; (3) 0.75; (4) 0.25.

Symmetry codes: (i) −x,−y + 1,−z + 2; (ii) −x + 2,−y,−z + 1; (iii) x−1, y, z + 1.

Journal of PeptideScience

higher thermal motion. Figure S2 in the Supporting Information shows the thermal ellipsoids.

Both chains adopt a regular 3_{10}-helical conformation stabilized by intramolecular hydrogen bonds with their torsion angles listed in Table 2. Eight consecutive H-bonds are formed starting from the carbonyl-group of the protection group and ending at the amino-group of Aib10 (Table 3).

In mol B, an additional H-bond is formed between the carboxyl-group of Aib10 and the C = O-group of Aib8, which leads to the formation of an oxy-analogue of a β-turn [29]. In the β-turn oxy-analogue of mol A, this H-bond is mediated by a co-crystallized, disordered water (OH-group of Aib10 to water 1 and water 1 to C = O-group of Aib8, Figure 1). This water molecule also forms an H-bond to the major component of the C = O-group of a symmetry related mol B. This can be seen in Table 2 and Figure 2. Water with smaller occupancy is found in the vicinity of Aib10 of mol B, 4.25 Å away from the first water molecule. This water is, similar to the first water, hydrogen bonded twice to mol B, namely to the C = O-group of Aib8 and to the minor component of the OH-group of Aib10. A third H-bond is formed with the symmetry related minor component of the C = O group of Aib10 of mol A. The helical parameters of the main backbone conformation of both molecules A and B were determined with the program *HELANAL* [30]. The average number of residues per turn is 3.22 and 3.15; the average rise per residue is 1.89 and 1.96 Å, and the average helical twist per residue is 111.7 and 114.4°, thus showing that molecule B is slightly more tightly wound than helix A.

The influence of the high resolution to the electron density maps was also investigated. The data were limited to a high resolution of 1.0 and 0.8 Å in the last cycles of refinement. The result is shown in the difference F_o-F_c maps in Figure 3. By decreasing the resolution limit, more details become visible, which are not explained by the usual spheric model of the atoms in the refinement program. At the sub-atomic resolution of 0.65 Å, the bonding electron density becomes visible between the non-hydrogen atoms.

The disorder at the termini of the molecules is more pronounced including the high resolution data (Supporting Information Figure S3).

In the crystal, one right-handed molecule A is head-to-tail hydrogen bonded to two left-handed molecules B, at the N-terminus with one H-bond (N1(A) to O9(B)) and at the C-terminus with two (N1(B) to O9(A) and N2(B) to O10(A)) (Table 3). Columns in the opposite crystal direction are formed between the left-handed molecules A and right-handed molecules B. The disordered 90% occupied water at the C-terminus of molecule A connects these columns via hydrogen bonds in such a way that always two antiparallel columns share the waters.

A one-molecule-layer of these planes built by the antiparallel columns is shown in Figure 2 viewed approximately along the diagonal [1 1 1]. Parallel to one layer (e.g. above and below the plane shown in Figure 2) are layers of columns of molecules of the same handedness consisting of the other molecules. These layers exhibit a shift of about three residues or one helical turn along the projection to the molecules in the layer in Figure 2.

The rings of the Z-protection group of both molecules are staggered in the crystal with average angle between the two planes of 10.6° for the first conformation of mol A and with 5.5° for the second conformation of molecule A. The average was performed between different atoms in both rings defining the plane (Table S1 of the Supporting Information).

The valence symmetry around the Cα atom is asymmetric for the Aib residues (Table 4 and Table S2). If one designates as CL and CR the atoms which occupy the same position as Cβ and α-hydrogen in L-amino acids respectively, the bond angles N-Cα-CL and C-Cα-CL are significantly smaller than the N-Cα-CR and the C-Cα-CR. This observation is in excellent agreement with theoretical calculations and with the bond angles of other right-handed 3_{10}-helical Aib-peptides [12,14].

Table 5 lists the helical parameters of the two herein described molecules (main conformations only) together with the closely

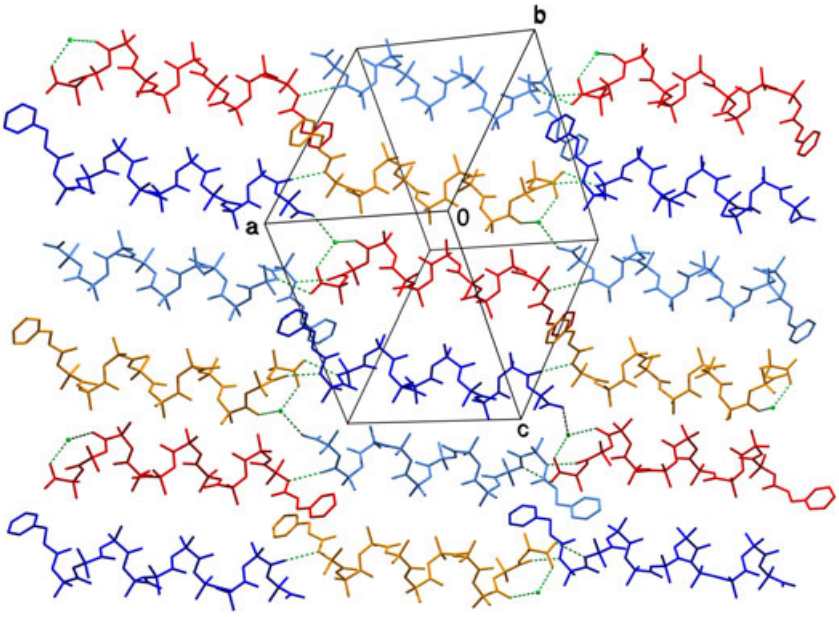

Figure 2. Crystal packing of Z-(Aib)$_{10}$-OH viewed approximately down the diagonal showing the infinitely long, antiparallel helical columns of alternating right-handed and left-handed molecules. Right-handed helices from molecules A are depicted in red, left-handed molecules A in orange; dark and light blue are the right-handed and left-handed helices of molecules B, respectively. The water molecules are shown as green spheres and the intermolecular hydrogen bonds as green dashed lines. For clarity, only the main conformations are shown.

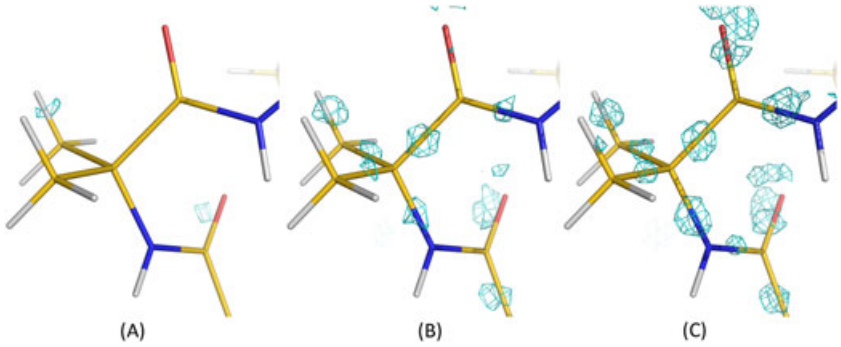

Figure 3. Electron density (cyan) around Aib7 of mol B. The F_o-F_c maps are contoured at 3σ (0.273 e Å^{-3}). The high resolution limit cut-off of the data is 1 Å (A), 0.8 Å (B) and 0.65 Å (C).

Table 4. Angles (°) defining the valence geometry around the Cα-atoms, average values of the main conformations

molecule	N-Cα-CL	C′-Cα-CL	N-Cα-CR	C′-Cα-CR
mol A	107.75(14)	107.12(15)	110.87(20)	110.56(19)
mol B	107.51(16)	107.15(16)	110.76(16)	109.90(16)

Table 5. Helical parameters for Z-(Aib)$_9$-O*t*Bu, Z-(Aib)$_{10}$-OH and Z-(Aib)$_{11}$-O*t*Bu. The parameters are derived from helices comprising all Aib-residues

Helix	Average number of residues/ turn	Average rise per residue [Å]	Average helical twist per residue [°]
Z-(Aib)$_9$-O*t*Bu mol A	3.21(11)	1.93(5)	112.0(3.9)
Z-(Aib)$_9$-O*t*Bu mol B	3.19(10)	1.94(5)	112.8(3.3)
Z-(Aib)$_{10}$-OH mol A	3.22(13)	1.89(8)	111.7(4.6)
Z-(Aib)$_{10}$-OH mol B	3.15(08)	1.96(5)	114.4(2.9)
Z-(Aib)$_{11}$-O*t*Bu	3.06(06)	1.97(4)	117.8(2.5)

related molecule Z-(Aib)$_{11}$-O*t*Bu [14] and the two independent molecules of Z-(Aib)$_9$-O*t*Bu (main conformation only) [12]. All of them deviate from the theoretical 3_{10}-helical values, which are 3.0 as average number of residues per turn and 120° as average helical twist per residue. The closest to the theoretical values are exhibited by the undecapeptide. This peptide possesses three complete turns, which seems to stabilize the internal structure. This is confirmed by thin layer chromatography experiments: in ethyl acetate (100%) and butyl acetate–methanol (98 : 2) the homopeptides with full turns (n = 5, 8, 11) and N-terminal Z protection and C-terminal O*t*Bu protection show relatively higher retention factor values compared with the homopeptides, which have one residue more or less [15]. In agreement, their melting point also shows higher values than the neighbouring peptides. Figure 4 shows a superposition of these five peptides. One can see that the three O*t*Bu protected molecules show a reversed backbone in the last residue, reflected by the opposite sign of the φ/ψ torsion angles. Z-(Aib)$_{10}$-OH does not reverse the backbone in the last residue and has the same sign of the φ/ψ torsion angles as the preceding residues (Table 2) and is therefore the only long Aib-homopeptide without a reversed helical sense in the last residue. Furthermore, counting the number of intramolecular hydrogen bonds, there are nine in mol B, and in mol A the ninth hydrogen bond is mediated by one water molecule. Nine is exactly the number of intramolecular hydrogen bonds in Z-(Aib)$_{11}$-O*t*Bu, and therefore, the shorter Z-(Aib)$_{10}$-OH has also three complete 3_{10}-helical turns.

Crystallization of partially protected peptides is facilitated by the possibility to form additional intermolecular hydrogen bonds as herein described. This makes the deprotection of peptides a method of choice in cases, where a fully protected peptide resists to form crystals suitable for X-ray analysis. Attempts are in progress in our lab to crystallize deprotected peptides derived from protected counterparts, which have never formed crystals to date.

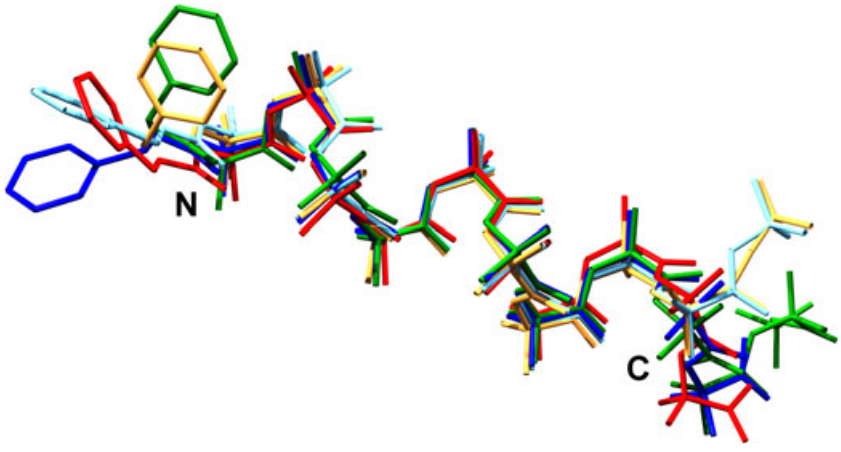

Figure 4. Least-squares superposition of the molecular structures of Z-(Aib)$_{11}$-O*t*Bu appear in green, Z-(Aib)$_{10}$-OH in red (mol A) and blue (mol B) and Z-(Aib)$_9$-O*t*Bu in yellow (mol A) and cyan (molB). For clarity, only the main conformations are shown.

Journal of PeptideScience

Acknowledgements

We are grateful to Dr Danny Axford, for assistance at the beamline I24 during data collection. The research leading to these results has received funding from the European Community's Seventh Framework Programme (FP7/2007-2013) under BioStruct-X (grant agreement N° 283570). This work was partly performed/conducted in the framework of the BIOSYS research project, Action KRIPIS, project no MIS-448301 (2013SE01380036) that was funded by the General Secretariat for Research and Technology, Ministry of Education, Greece, and the European Regional Development Fund (Sectoral Operational Programme: Competitiveness and Entrepreneurship, NSRF 2007–2013)/European Commission.

References

1 Karle IL, Flippen-Anderson JL, Sukumar M, Balaram P. Aqueous channels within apolar peptide aggregates: solvated helix of the α-aminoisobutyric acid (Aib)-containing peptide Boc-(Aib-Ala-Leu)3-Aib-OMe •H2O•CH3OH in crystals. *Proc. Natl. Acad. Sci. U. S. A.* 1988; **85**: 299–303.
2 Chugh JK, Brückner H, Wallace BA. Model for a helical bundle channel based on the high-resolution crystal structure of trichotoxin_A50E. *Biochemistry* 2002; **41**: 12934–12941.
3 Gessmann R, Axford D, Evans G, Brückner H, Petratos K. The crystal structure of samarosporin I at atomic resolution. *J. Pept. Sci.* 2012; **18**: 678–684.
4 Sansom MSP. Structure and function of channel forming peptaibols. *Quart. Rev. Biophys.* 1993; **26**: 365–421.
5 Toniolo C, Valle G, Bonora GM, Crisma M, Formaggio F, Bavoso A, Benedetti E, Di Blasio B, Pavone V, Pedone C. A novel peptide conformation: first unequivocal observation of the oxy-analog of a β-bend. *Biopolymers* 1986; **25**: 2237–2253.
6 Benedetti E, Bavoso A, Di Blasio B, Pavone V, Pedone C, Crisma M, Bonora GM, Toniolo C. Solid-state and solution conformation of homo oligo(α-aminoisobutyric acids) from tripeptide to pentapeptide: evidence for a 3_{10}-helix. *J. Am. Chem. Soc.* 1982; **104**: 2437–2444.
7 Shamala N, Nagaraj R, Balaram P. The 3_{10}-helical conformation of a pentapeptide containing α-aminoisobutyric acid (Aib): X-ray structure of Tos-$(Aib)_5$-OMe. *J. Chem. Soc. Chem. Commun.* 1978; **996–997**.
8 Vlassi M, Brückner H, Kokkinidis M. The crystal structure of the conformationally constrained peptide Z-(Aib)6-OBu^t. *Zeit. Kristallogr.* 1992; **202**: 89–98.
9 Pavone V, Di Blasio B, Pedone C, Santini A, Benedetti E, Formaggio F, Crisma M, Toniolo C. Preferred conformation of homo-oligomers of α-aminoisobutyric acid: molecular and crystal structure of Z-$(Aib)_7$-OMe. *Gazz. Chim. Ital.* 1991; **121**: 21–27.
10 Vlassi M, Brückner H, Kokkinidis M. Peptide with built in constraints: structure of Z-$(Aib)_7$-OtBu. *Acta Crystallogr.* 1993; **B49**: 560–564.
11 Bavoso A, Benedetti E, Di Blasio B, Pavone V, Pedone C, Toniolo C, Bonora GM. Long polypeptide 3_{10}-helices at atomic resolution. *Proc. Natl. Acad. Sci. U. S. A.* 1986; **83**: 1988–1992.
12 Gessmann R, Brückner H, Kokkinidis M. Structure of Z-$(Aib)_9$-OBu^t. *Acta Crystallogr.* 1998; **B54**: 300–307.
13 Toniolo C, Crisma M, Bonora GM, Benedetti E, Di Blasio B, Pavone V, Pedone C, Santini A. Preferred conformation of the terminally blocked $(Aib)_{10}$ homooligopeptide: a long regular 3_{10}-helix. *Biopolymers* 1991; **31**: 129–138.
14 Gessmann R, Brückner H, Petratos K. Three complete turns of a 3_{10}-helix at atomic resolution: the crystal structure of Z-$(Aib)_{11}$-OtBu. *J. Pept. Sci.* 2003; **9**: 753–762.
15 Brückner H. Oxazolone activation in the synthesis of oligopeptides containing α-methylalanine. In *Chemistry of Peptides and Proteins*, Vol. **4**, Koenig WA, Voelter W (eds). Attempto Verlag: Tuebingen, 1989; 79–86.
16 Theis C, Degenkolb T, Brückner H. Studies on the selective trifluoroacetolytic scission of native peptaibols and model peptides using HPLC and ESI-CID-MS. *Chem. Biodivers.* 2008; **5**: 2337–2355.
17 Evans G, Axford D, Owen RL. The design of macromolecular crystallography diffraction experiments. *Acta Crystallogr.* 2011; **D67**: 261–270.
18 Kabsch W. *XDS. Acta Crystallogr.* 2010; **D66**: 125–132.
19 Evans PR, Murshudov GN. How good are my data and what is the resolution? *Acta Crystallogr.* 2013; **D69**: 1204–1214.
20 Winn MD, Ballard CC, Cowtan KD, Dodson EJ, Emsley P, Evans PR, Keegan RM, Krissinel EB, Leslie AG, McCoy A, McNicholas SJ, Murshudov GN, Pannu NS, Potterton EA, Powell HR, Read RJ, Vagin A, Wilson KS. Overview of the CCP4 sui and current developments. *Acta Crystallogr.* 2011; **D67**: 235–242.
21 Sheldrick GM. A short history of Shelx. *Acta Crystallogr.* 2008; **A64**: 112–122.
22 McRee DE, Israel M. XtalView, protein structure solution and protein graphics, a short history. *J. Struct. Biol.* 2008; **163**: 208–213.
23 Guex N, Peitsch MC. SWISS-MODEL and the Swiss-PDBViewer: an environment for comparative protein modeling. *Electrophoresis* 1997; **18**: 2714–2723.
24 Emsley P, Lohkamp B, Scott WG, Cowtan K. Features and Development of Coot. *Acta Crystallogr.* 2010; **D66**: 486–501.
25 Burnett MN, Johnson CK. ORTEPIII: Oak Ridge thermal ellipsoid plot program for crystal structure illustrations. Report ORNL-6895, Oak Ridge National Laboratory, Tennessee, USA, 1996.
26 DeLano WL. The *PyMOL* Molecular Graphics System, 2002. Available at: http://www.pymol.org [accessed August 2015].
27 Persistence of Vision Pty Ltd, 2004. Available at: http://www.povray.org [accessed August 2015].
28 Groom CR, Allen FH. The Cambridge Structural Database in retrospect and prospect. *Angew. Chem. Int. Ed.* 2014; **53**: 662–671.
29 Benedetti E, Bavoso A, Di Blasio B, Pavone V, Pedone C, Toniolo C, Bonora GM. First observation of a β-turn conformation fused with the oxy-analogue of an α-turn: the molecular structure of a model peptide of the C-terminal part of gramicidin A. *Biochem. Biophys. Res. Commun.* 1983; **112**: 1056–1060.
30 Bansal M, Kumar S, Velavan R. HELANAL: a program to characterize helix geometry in proteins. *J. Biomol. Struct. Dyn.* 2000; **17**: 811–819.

Supporting Information

Additional supporting information may be found in the online version of this article at the publisher's web site.

